

行政院國家科學委員會專題研究計畫 成果報告

慣質之觀念及控制之應用

計畫類別：個別型計畫

計畫編號：NSC92-2218-E-002-052-

執行期間：92年12月01日至93年07月31日

執行單位：國立臺灣大學機械工程學系暨研究所

計畫主持人：王富正

共同主持人：游忠煌

計畫參與人員：張孟倫、徐茂盛

報告類型：精簡報告

處理方式：本計畫可公開查詢

中 華 民 國 93 年 10 月 28 日

行政院國家科學委員會專題研究計畫成果報告

慣質之觀念及控制之應用 Inerter Concepts and its Applications

計畫編號：NSC92-2218-E-002-052
執行期限：92年12月01日至 93年07月31日

主持人： 王富正* 國立臺灣大學機械工程學系暨研究所
共同主持人：游忠煌 陽明大學復健科技輔具研究所
計畫參與人員：張孟倫、徐茂盛 國立臺灣大學機械工程學系暨研究所

Abstract

This paper discusses the concepts of a newly-developed mechanical network element, called *Inerter*, and its applications to the train suspension system. It begins with the detailed description of *Inerter* and its realizations, followed by applications to train suspension control. A parallel combination of *Inerter* with a traditional suspension strut is constructed and tested.

Keywords: Inerter, Networks, suspension

中文摘要

本論文討論一個新的機械元件-慣質-的觀念，以及它在火車懸吊的應用。在實驗方面，我們組裝了一個慣質機構，並且將它與傳統的懸吊作並聯式的組合，應用系統識別的方式去驗證它的性質。

1. Introduction

It is well known that two analogies, namely the *force-voltage* and *force current* analogies, exist between the mechanical and electrical systems. These can be easily derived from the dynamic equations of the traditional mechanical and electrical systems.

A *force-current* analogy is presented in Table 1, where the mechanical elements, mass (m), damper (c) and spring (k) are analog to the electrical elements, capacitor (C), inductor (L) and resistor (R) respectively.

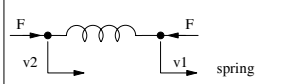
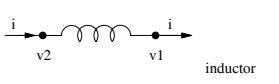
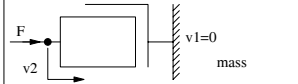
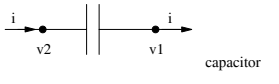
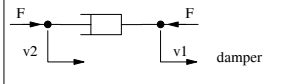
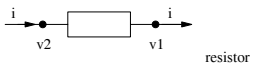
Mechanical	Electrical
 spring	 inductor
 mass	 capacitor
 damper	 resistor

Table 1. The traditional (*force-current*) analogy between mechanical and electrical systems.

As noticed in Table 1, the mass (m) in mechanical systems is not truly analog to the capacitor (C) in electrical systems in that one of its two ports **must** be grounded. As a result, it put extra limitation on the achievable performance of passive mechanical network systems. That is, some passive networks cannot be realized by the traditional passive mechanical elements, though they can be realized by the passive electrical elements.

It is from the observation of Table 1 that the *Inerter* concept was proposed. A new mechanical/electrical analogy is illustrated in Table 2, where *Inerter* is a true analogy to a capacitor. The dynamic equation of *Inerter* can be expressed as follows:

$$F = b \frac{d(v_2 - v_1)}{dt}$$

in which v_1 and v_2 represent the velocities of the two ports of the *Inerter*.

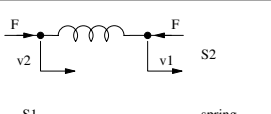
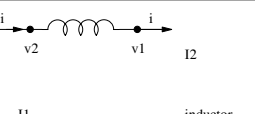
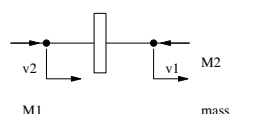
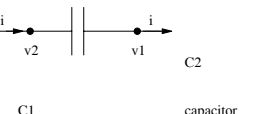
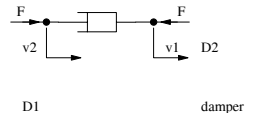
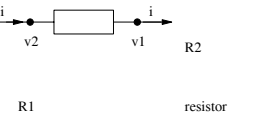
Mechanical	Electrical
 <p>S2 S1 spring</p>	 <p>I2 I1 inductor</p>
 <p>M2 M1 mass</p>	 <p>C2 C1 capacitor</p>
 <p>D2 D1 damper</p>	 <p>R2 R1 resistor</p>

Table 2. The new analogy between mechanical and electrical systems.

2. Applications of *Inerter* to train suspension control

In this section, we apply *Inerter* to train suspension control, and discuss the potential performance improvements. A traditional one-wheel train model is shown in Figure 1, where m_s , m_b , m_w represent the masses of the train body, bogie and wheel respectively. The traditional train suspension design is to add a damper c_s and a spring k_s between the train body and bogie, and to add a damper c_b and a spring k_b between the bogie and wheel, with the wheel itself modeled as a parallel combination of a damper c_w and a spring k_w . The following parameters are chosen for a standard one-wheel train model:

$$m_s=3500 \text{ kg}; m_b=250 \text{ kg}; m_w=350 \text{ kg};$$

$$c_s=8870 \text{ Ns/m}; c_b = 7100 \text{ Ns/m}; c_w = 670 \times 10^3 \text{ Ns/m};$$

$$k_s=141 \text{ kN/m}; k_b=1260 \text{ kN/m}; k_w=8000 \times 10^3 \text{ kN/m}.$$

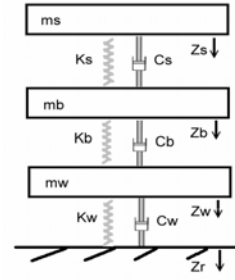


Figure 1. The one-wheel train model.

Performance Indexes

Many indexes can be used to investigate the performance of the suspension control systems. Among them, the most commonly used are the system minimal damping ratio, J_1, J_3, J_5 , which represent the system ability of anti-vibration, the ride comfort, the dynamic wheel load and the suspension load ability respectively, expressed as follows:

$$J_1 = \left\| s \cdot T_{z_r \rightarrow z_s} \right\|_2; J_3 = \left\| \frac{1}{s} \cdot T_{z_r \rightarrow F_r} \right\|_2; J_5 = \left\| s \cdot T_{F_s \rightarrow z_s} \right\|_\infty.$$

Suspension layouts

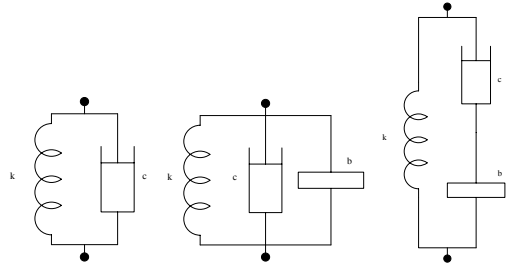


Figure 2. The traditional suspension, the parallel, and the serial arrangements (from left).

Three suspension layouts are considered, namely the traditional, the parallel and the serial arrangements, as shown in Figure 2. Furthermore, it is noticed that the *Inerter* can be added with c_s and k_s between the train body and the bogie, or with c_b and k_b

between the bogie and the wheel. We will discuss both of the cases.

Inerter between train body and bogie

Now we discuss the scenario of adding *Inerter bs* with c_s and k_s . Firstly we look for the optimal damping ratio by adjusting parameters at every fixed stiffness k_s . That is, we are looking for the optimal settings of b_s, c_s to achieve:

$$\max_{b_s, c_s}(\zeta_{\min})$$

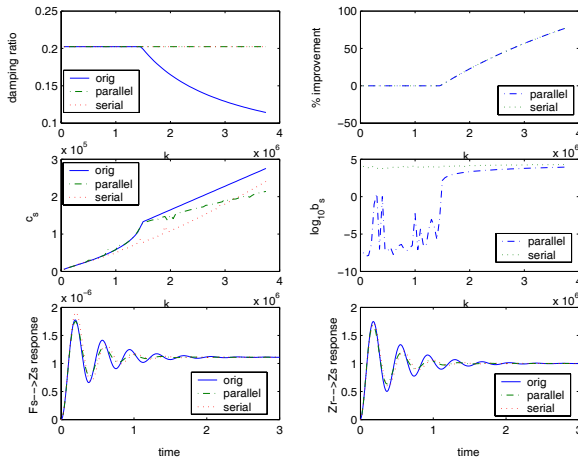


Figure 3. Improvement of optimal damping ratio by *Inerter* between the train body and the bogie.

For example, when $k_s = 3150$ kN/m, the optimal damping ratio is $\zeta = 0.12563$ with $c_s = 237.35$ kNs/m for the traditional suspension. And the damping ratio can be improved to $\zeta = 0.20231$ with the parallel arrangement ($b_s = 6501.3$ kg, $c_s = 193.27$ kNs/m) or the serial arrangement ($b_s = 19289$ kg, $c_s = 193.56$ kNs/m). A complete analysis for various stiffness k_s is illustrated in Figure 3. It is noticed that there is a performance gain up to 60 % with *Inerter* in both of the serial and parallel arrangements. The time responses of the last two plots of Figure 3 is based on the above data when $k_s = 3150$ kN/m. Similarly, we could optimize

the parameters over other performance indexes, J_1, J_3, J_5 , as listed in Table 3.

	traditional	parallel	serial
ζ_{\min}	$k_s = 2.25 \times 10^6$	2.25×10^6	2.25×10^6
	$\zeta_{\min} = 0.15316$	0.20231	0.20231
	% improvement	32.09%	32.09%
	$C_s = 1.8039 \times 10^5$	1.6034×10^5	1.2511×10^5
	$b_s = 0$	3080.3	14464
J_1	$k_s = 2.25 \times 10^6$	2.25×10^6	2.25×10^6
	$J_1 = 100.64$	100.52	87.872
	% improvement	0.12%	12.69%
	$C_s = 1.0381 \times 10^5$	1.0426×10^5	1.5081×10^5
	$b_s = 0$	7.5873	1.0127×10^4
J_3	$k_s = 1.25 \times 10^6$	1.25×10^6	1.25×10^6
	$J_3 = 34019$	32714	32553
	% improvement	3.84%	4.31%
	$c_s = 9.6999 \times 10^4$	6.3885×10^4	1.5095×10^5
	$b_s = 0$	3.2714×10^4	3.2553×10^4
J_5	$k_s = 1.25 \times 10^6$	1.25×10^6	1.25×10^6
	$J_5 = 2.83 \times 10^6$	1.7166×10^6	2.1961×10^6
	% improvement	39.34%	22.46%
	$c_s = 1.7898 \times 10^5$	1.6079×10^5	1.78260×10^5
	$b_s = 0$	7.4473×10^3	3.453×10^4

Table 3. Performance improvement by *Inerter* between the train body and bogie.

Inerter between bogie and wheel

We now discuss the scenario of adding *Inerter bb* with cb and kb . Similar results can be derived, as shown in Figure 4. The time responses are based on the optimal setting when $kb = 1800$ kN/m, where with $cb = 487.68$ kNs/m it achieves $\zeta = 0.21168$ for the traditional suspension. For the serial arrangement with $cb = 399.33$ kNs/m and $bb = 61873$ kg it achieves $\zeta = 0.31595$, a 49.26%

improvement. It is noticed that the parallel arrangement does not give performance gain at this place.

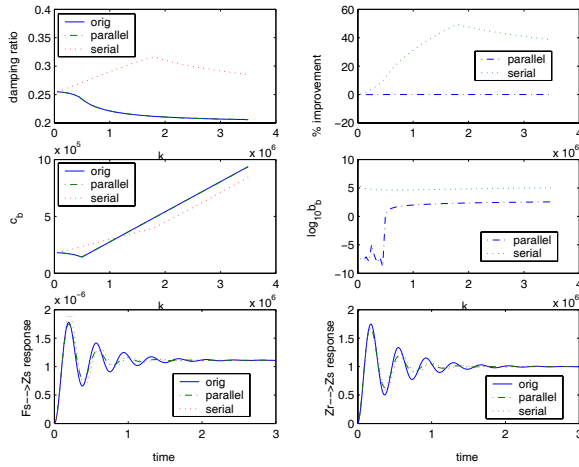


Figure 4. Improvement of optimal damping ratio by *Inerter* between bogie and wheel.

Similarly, we also optimize the system over various performance indexes J_1, J_3, J_5 . The results are listed in Table 4.

	traditional	parallel	serial
ζ_{\min}	$\zeta_{\min} = 0.21168$	0.21173	0.31595
	% improvement	0.001%	49.53%
	$c_b = 4.8768 \times 10^5$	4.8701×10^5	3.9933×10^5
	$b_b = 0$	207.44	6.1873×10^4
J_1	$J_1 = 26.788$	26.741	25.92
	% improvement	0.18%	3.24%
	$c_b = 1.357 \times 10^4$	1.3501×10^4	1.6903×10^4
	$b_b = 0$	1.9121	275.106
J_3	$J_3 = 2.9791 \times 10^4$	2.9791×10^4	2.9216×10^4
	% improvement	0%	1.93%
	$c_b = 1.9386 \times 10^5$	1.9386×10^5	1.1632×10^4
	$b_b = 0$	1.31×10^{-11}	2.3121×10^{13}
J_5	$J_5 = 1.7752$	$4021 \cdot 10^{-5}$	$4608 \cdot 10^{-5}$
	% improvement	21.02%	17.71%
	$c_b = 946350$	162670	1082900
	$b_b = 0$	74593	89640

Table 4. Performance improvement by *Inerter* between bogie and wheel.

3. The realization of *Inerter* concepts

With the *Inerter* concept, the first *Inerter* model in Taiwan is assembled, as shown in Figure 5. Based on this model, an experimental model was made in the department factory with inertance $b = 147.65692$ Kg, while itself weights only about 3 Kg. Since *Inerter* is a new idea (proposed in 2001), there is no commercial model at all. Consequently, every model must be built in house.

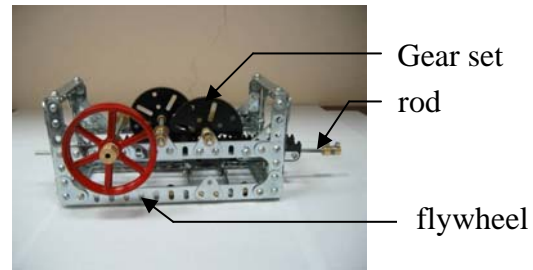


Figure 5. The first *Inerter* model in Taiwan.

Experiment design

The purpose of the experiments is to verify the *Inerter* properties. For this experiment, *Inerter* is combined in parallel with a traditional suspension strut, as shown in Figure 6, with damping rate $c = 220$ Ns/m and spring stiffness $k = 33$ kN/m.

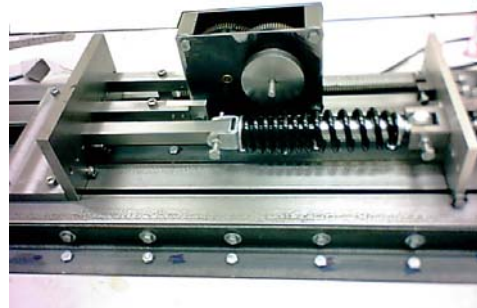


Figure 6. A parallel arrangement strut.

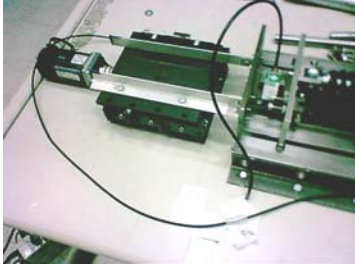


Figure 7. The experiment platform.

For system identification purposes, the platform is given a sinusoidal reference, while the strut displacement and force are recorded by a position sensor and a load cell, as shown in Figure 8. The position sensor measures in the unit of $1 \mu\text{m}$, while the load cell reading is in the unit of 24.4 g (with a 12 bits DAQ card) with a limit of 100 Kg .

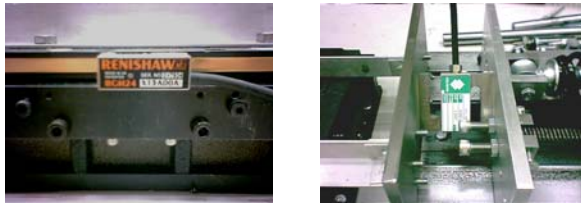


Figure 8. The position sensor and the load cell.

System identification

The system identification techniques from [3] are adapted to verify the *Inerter* properties. Considering a system $G(s)$ with input u and output y , i.e. $Y(s) = G(s)U(s)$, where s means the Laplace Transform of the signals. If the input is given as $u(t) = \alpha \cos(\omega t)$, then the gain and phase of the system can be obtained by measuring the output $y(t)$ and processing as follows:

$$I_c = \frac{1}{N} \sum_{t=1}^N y(t) \cos(\omega t), \quad I_s = \frac{1}{N} \sum_{t=1}^N y(t) \sin(\omega t),$$

$$|G(j\omega)| = \frac{\sqrt{I_c^2 + I_s^2}}{\alpha/2},$$

$$\angle G(j\omega) = -\tan^{-1}\left(\frac{I_s}{I_c}\right).$$

Experimental results

For the experimental strut, the transfer function from the displacement to force is

$$G(s) = \frac{F(s)}{U(s)} = bs^2 + cs + k,$$

with $s = j\omega$. Theoretically the magnitude and phase of the transfer function are:

$$|G(j\omega)| = \sqrt{(k - b\omega^2)^2 + c^2\omega^2}, \quad \angle G(j\omega) = \tan^{-1}\left(\frac{c\omega}{k - b\omega^2}\right).$$

The experimental results will be compared with the theoretical values and verified. We use LabView to control the movement of the platform, and to record the displacement and force signals from the position sensor and load cell. A typical record of the reference, actual displacement and force signals is illustrated in Figure 9, with $\omega = 2\pi$ (1 Hz), and $\alpha = 5 \text{ mm}$.

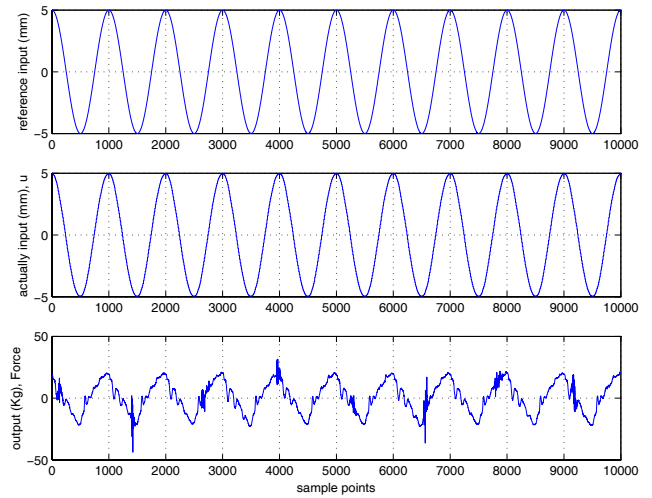


Figure 9. The reference, actual displacement and force signals, in the units of mm and Kgw.

Similar experiments were carried out for various frequencies at 1, 2, 3, 4, 5, 6, 8, 10, 12, 14, 16Hz, and the corresponding magnitudes were adjusted not to exceed the working range of the load cell. It is noticed that the force increases dramatically as the frequency increases, due to the term bs^2 in the transfer function. The experimental

results are compared with the theoretical values, as illustrated in Figure 10. It is noticed that the properties of the working strut fits very well in the low frequency range. At high frequency, the disagreement of the experimental and theoretical values may be resulted from the limitation on the magnitude of displacement signals (so that the noise-signal ratio may be too high) and the practical mechanical problems, such as friction, backlash e.t.c.

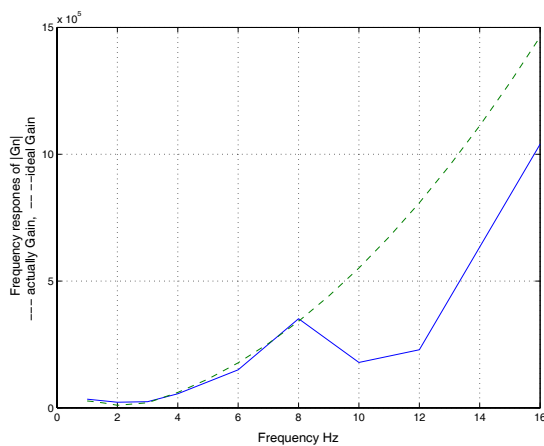


Figure 10. $|G(j\omega)|$ from the experimental data (solid) and the theoretical value (dashed).

4. Concluding remarks

This paper has discussed the *Inerter* concepts in details and applied it into the train suspension design. It was concluded that the system performance can be generally improved with *Inerter* in the system design. From the simulations of train suspensions, it was also noticed that some *Inerter* layouts might be more suitable for particular performance requirement than others. The experiment was carried out to verify the *Inerter* properties. This work will be continued in different angles. We are now looking for the potential performance benefits of *Inerter* in vehicle systems, and the

general realization of passive network by *Inerter*. In the end, it should be noted that *Inerter* is a new general mechanical element, and has the potential to improve performance for general engineering systems, such as the anti-vibration design for the buildings in civil engineering.

Reference

1. E.L. Hixson, *Mechanical Impedance shock and vibration Handbook*, 2nd edition, C.M. Harris, C.E. Crede (Eds.), Chapter 10, McGraw-Hill, 1976.
2. C. G. Koh, J. S. Y. Ong, D. K. H. Chua and J. Feng. *Moving element method for train-track dynamics*. Int. J. Numer. Meth. Engng. 2003; 56: 1549-1567
3. L. LJUNG. *System identification: theory for the user*. 1999. Prentice Hall PTR.
4. J.L. Shearer, A.T. Murphy and H.H. Richardson, *Introduction to system dynamics*, Addison-Wesley, 1967.
5. M.C. Smith and F.-C. Wang. *Performance Benefits in Passive Vehicle Suspensions Employing Inerters*. 42nd IEEE Conference on Decision and Control, Hawaii, USA, December 9-12, 2003.
6. M.C. Smith. *Synthesis of mechanical networks: the inerter*. IEEE Transactions on Automatic Control}, 47, 1648-1662, 2002.